

Ocean wave nonlinearity and phase couplings

M J Varkey

National Institute of Oceanography, Dona Paula, Goa 403 004, India

Received 10 May 1990; revised 8 April 1991

Bispectrum of a swell dominated sea state is computed using Fourier coefficients from an original record and from simulated Fourier coefficients using pseudorandom (uniform) phase spectrum. The differences in the bispectra clearly bring out the effect of phase couplings or phase relationships in forming nonlinear characteristics of the sea state. Even in the very mildly nonlinear sea state, the phase spectral values are related as in Stokes waves. Nonlinear activity in a sea state depends also on presence and intensity of nonlinear component waves.

The generally observed surface waves in the sea are caused by wind and form a separate group of about 0.1 to 60 sec periods; the lowest periods constitute capillary waves and the highest periods arise out of presence of wave groups. Wind waves are formed and grown at the sea surface by continued action of wind through its force pulses of different durations, instantaneous or sustained, from the initial capillaries to the fully developed giant waves; the nature and dominance of the forcing pulses changing with the growth of wind. If the process of initial wave generation is monitored on the water surface from a single force pulse, it can be seen that the sea surface is disturbed always by wavelets and their groups. Over the surface the force pulses are innumerable, spread over a very wide area.

and of different natures like instantaneous pushes by normal pressure components, horizontal thrusts by tangential forces and sustained energy inputs by mean wind.

Out of the many models of waves, Airy's, Cnoidal and Stokes' are approximate solutions for very regular and periodic sea waves, while the Fourier theory models accurately a narrow band sea state with many component waves (CW, Fig. 1C) and with a phase spectrum generally considered to be uniformly random. But a fully uniform-random phase spectrum is realisable only from an ideal linear stochastic system. In all other cases (all sea states) wherein a Fourier transform is applicable, there would exist mild or strong phase couplings or alignments depending

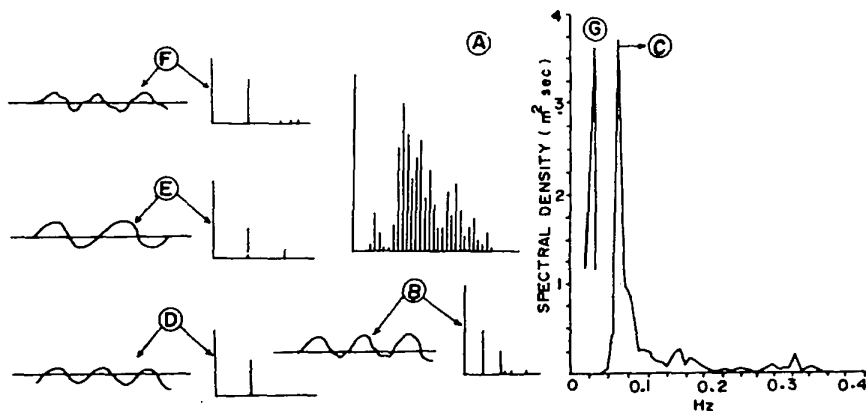


Fig. 1—Different wave forms and their raw spectra (schematic) with the smoothed spectrum (C) of the sea state under study; (A)—raw line spectrum of a typical sea state; (B), (F)—nonlinear Stokes wave and Sine wave with deformations; (D)—Sine wave, and (E)—nonlinear Stokes wave. Suspended single peak (G) is from a sinusoidal profile to show the resolution of CW peaks

upon the overall nonlinearity of the sea state. It seems that the amplitude and nonlinearity of the CW would increase with the duration of the forcing pulses. Hence, the nonlinearity of the CW and the sea state can be expected to be large when the energy input from the wind by the coupled mode is at a maximum and during breaking. Correspondingly, the nonlinearity of the CW (almost linear) and sea state would be a minimum during the initial phase of wave generation. But, the Traditional Linear Spectrum (TLS) alone fails to resolve or identify the nonlinear CW in a sea state (Fig. 1A, F).

Various wave forms and their raw line spectra show that deformations on the sea surface give rise to additional spectral lines (Fig. 1B, F) in the cases of regular nonlinear and linear waves, respectively, when they are mildly distorted. This effect can be largely caused by shearing and tangential stress on the sea surface which do not cause wavy propagating disturbances but only horizontal deformations like vertically asymmetrical waves. Spurious (in the sense extra or additional) spectral lines were first noted by Lake and Yuen¹ in their numerical studies on evolution of nonlinear wave trains and they have not been given adequate importance in studying nonlinear aspects of sea states. For these spurious spectral lines, the associated phase values do not hold much sense. Hence, the phase spectrum can contain spurious values with no

physical significance in addition to real coupled related phases of strongly nonlinear CW and almost independent values associated with almost linear CW. As these aspects are not given much attention, a numerical experiment is carried out on a very narrow band sea state (Fig. 1C) resulting in original and simulated bispectra bringing out the effect of phase couplings in an ordinary sea state.

Materials and Methods

The wave data were recorded using a ship-borne wave recorder at a deep water station (> 250 m) in the Bay of Bengal². A total record length of 768 sec resulting in 6 sub-profiles of 128 digitised values at 1 sec intervals was used for the computation. The bispectrum is computed using an expression as given by Kim and Powers³.

$$B(k, l) = \frac{1}{M} \sum_{i=1}^M X_i(k) X_i(l) X_i^*(m)$$

where m is $k+l$; $B(k, l)$, an estimator of bispectrum; M , number of sub-profiles; k, l and m are frequencies of interacting CW; and $X(k), X(l)$ and $X(m)$, complex, raw Fourier coefficients. The methodology was found⁴ to give good results enabling original interpretations of bispectrum of waves. In the case of simulation, $X(k), X(l)$ and $X(m)$ are recomputed using pseudo-

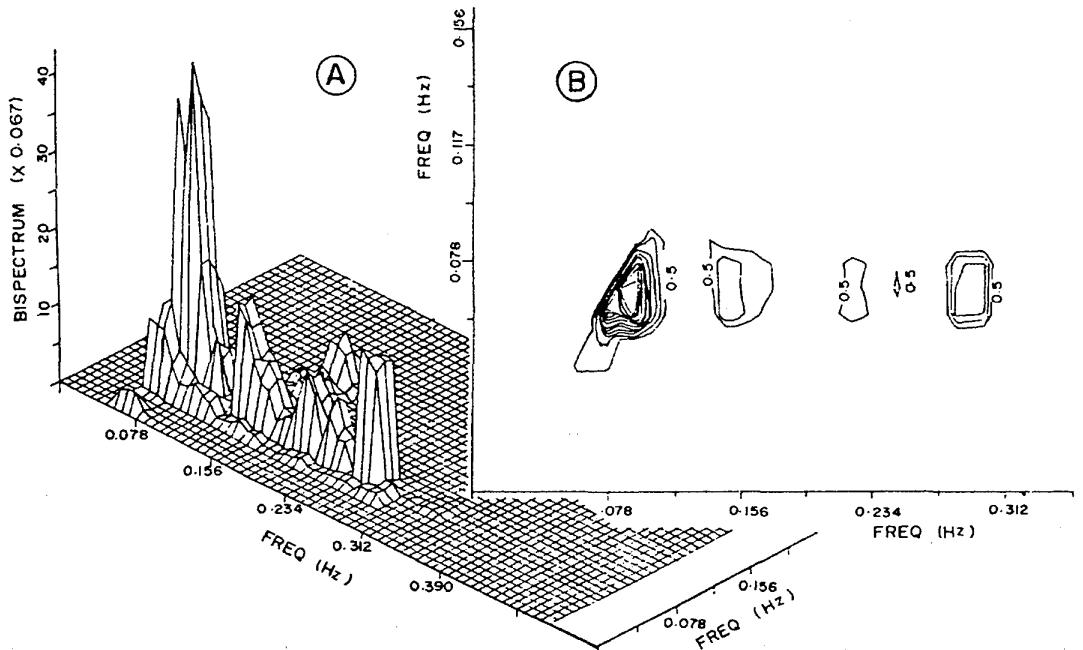


Fig. 2—Bispectrum in 2 formats of the sea state under study (contouring interval is 0.25)

random uniform phases after discarding the original coupled phase values. These recomputed (linearised) Fourier coefficients are used to calculate the bispectrum which would be free from the effects of natural phase couplings.

Results and Discussion

Figs 2 and 3 show the original and simulated bispectra (in 2 formats) of the same autospectrum as shown in Fig. 1C. The 3-dimensional figures obscure some of

the quantitative aspects. Hence, some of the features are quantitatively delineated from the figures and are presented in Table 1.

As the simulated phase spectral change to pseudorandom uniform values does not affect the autospectrum (Fig. 1C) except for a change from nonlinear to linear CW, the autospectral characteristics entered in Table I against recorded and simulated cases (I and II) are the same. One conspicuous feature to be noted in the autospectrum is its maximum at 0.065 Hz con-

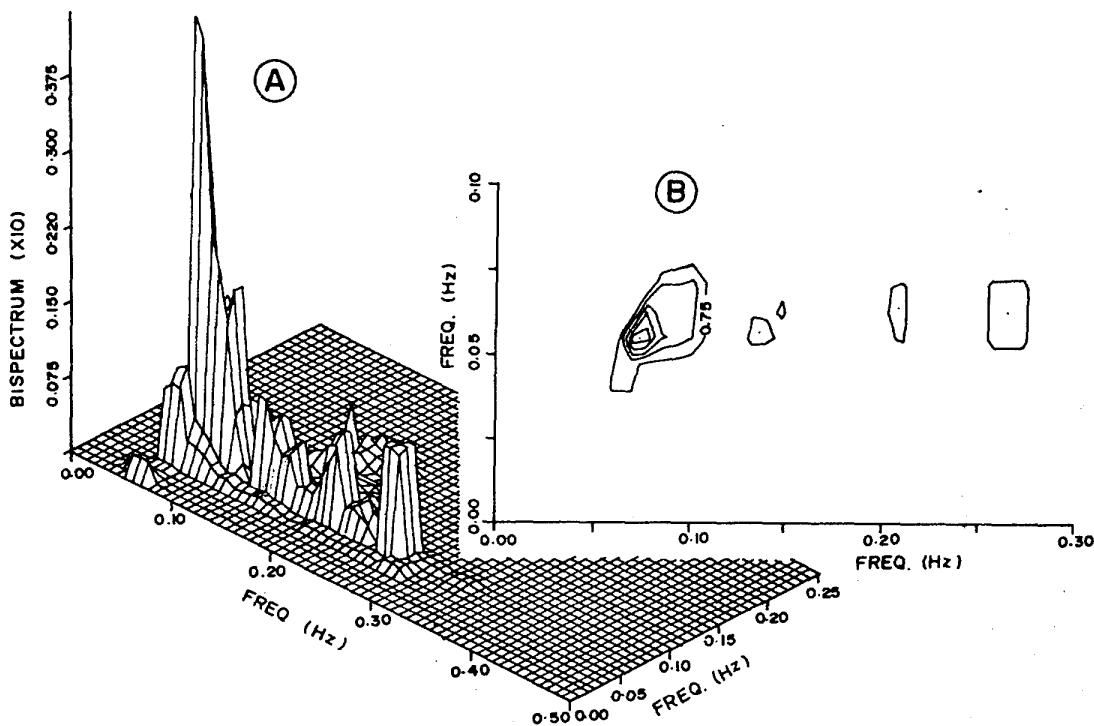


Fig. 3—Simulated bispectrum using uniform pseudorandom phase spectrum and the original autospectrum (contouring interval is 0.75)

Table 1—Bispectral and autospectral features derived from recorded profile and simulated Fourier coefficients using uniform pseudorandom phases

Fourier coefficients	Bispectral peaks			Autospectral peaks				Approx noise level (m ³ sec ²)	Bispectral vol	
	X-freq	Y-freq	Intensity	Harmonic-related freq	Intensity (m ² .sec)	Other freq	Intensity (m ² .sec)		Real	Imag
From recorded profile I	0.092	0.066	2.9	0.065	3.7	0.078	0.8	0.8	-0.0109	-0.0136
	0.290	0.066	> 1.0	0.140	0.3	0.094	0.25			
	0.150	0.066	> 0.7	0.206	< 0.1	0.159	0.20			
	0.220	0.066	> 0.5			0.228	< 0.1			
	0.250	0.066	> 0.5			0.275	~ 0.1			
Simulated II	0.072	0.056	4.4	0.065	3.7	0.078	0.8	0.9	+0.0061	+0.0121
	0.14	0.056	> 0.7	0.140	0.3	0.094	0.25			
	0.21	0.065	> 0.7	0.206	< 0.1	0.159	0.20			
	0.27	0.063	> 0.7			0.228	< 0.1			
						0.275	~ 0.1			

stituted by a single nonlinear CW. But the complete range from 0.065 to 0.094 Hz has interaction significance as evidenced in the wide cross section of the primary bispectral peak (Fig. 2). (The bispectral cross-section obtained for a sinusoidal wave using the same computing algorithm is only about 1/3 of this size). The noise levels in both the bispectra (Figs 2 and 3) are approximately same; the minor difference being due to the large primary peak of 4.4 in the case of II. The wide bispectral peaks in Fig. 2 include higher harmonics (0.14 and 0.206 Hz) of the main CW peak at 0.065 Hz or low amplitude nonlinear CW at 0.078, 0.094, 0.159 and 0.228 Hz. The largest and widest bispectral peak at (0.092, 0.066) includes a peak-to-peak interaction centered around (0.065, 0.065) and interactions of minor nonlinear CW centered at 0.078 and 0.094 Hz. Since the maximum is centered at (0.092, 0.066) the low amplitude CW at 0.094 Hz seems to be highly nonlinear compared to even the highest CW at 0.065 Hz. The second largest peak (Fig. 2) at (0.29, 0.066) seems to be the third harmonic contribution from the CW at 0.094 Hz whose second harmonic contribution is clubbed with the peak at (0.15, 0.066).

Even though the simulated bispectrum (Fig. 3) superficially looks the same as the real (Fig. 2), its characteristics differ significantly bringing out the effect of phase couplings in the real case. Firstly, the apparent similarity of the same number of harmonic peaks situated similarly is superficial, since all the subpeaks in Fig. 3 are below the approximate noise level of $0.9 \text{ m}^3\text{sec}^2$. But the subpeak in Fig. 2 at (0.29, 0.066) is well above the noise level of $0.8 \text{ m}^3\text{sec}^2$ and the one at (0.15, 0.066) cannot be ruled out as insignificant since the specified noise level is only approximate and real sea state is always nonlinear. The bispectral intensity depends on amplitudes and phase and frequency relations of CW in interaction. Hence, increased intensities at (0.29, 0.066) and (0.15, 0.066) in Fig. 2 are due to phase couplings between the CW at 0.094 Hz and its second and third harmonics and the CW at 0.078 Hz and its second harmonic. The absence of significant peaks for the higher harmonics of 0.078 and 0.094 Hz in Fig. 3 clearly brings out the existence of phase couplings

even in a very mildly nonlinear sea state with only one dominant swell CW, the nonlinear CW at 0.078 and 0.094 Hz being only about 1/10th of the largest CW and the mean high frequency ($> 0.15 \text{ Hz}$) CW intensity being only about 1/30th. The striking feature is that, maximum nonlinear intensity for the CW is at 0.094 Hz and not for the largest CW at 0.065. Another effect of phase couplings in the spectral peak regime alone is the shift of the bispectral peak from (0.092, 0.066) in case I to (0.072, 0.056) in case II. In case of I the effect is due to the large nonlinearity of the CW at 0.094 Hz compared to the peak CW at 0.065 and 0.078 Hz. In case II, with simulated phase values, Stokes type nonlinearity of the CW in the peak regime is removed. Hence, the bispectral peak is due to only the large amplitude of the CW at 0.065 Hz (by self interaction). This explains the shift of the peak to (0.072, 0.056) and the increase to 4.4 from 2.9. The transformed peak's (case II) placement at (0.072, 0.056) in Fig. 3, instead at (0.065, 0.065), is due to its steep and asymmetric nature and specification at centre of highest contour. In case II, self interaction peaks of the linearised CW at 0.078 and 0.094 Hz merge between the contours of 1.5 and 2.25 (Fig. 3B) with the peak of the linearised CW at 0.065 Hz, but can be seen separately in Fig. 3A. The effect of simulation is strikingly seen in changes in volumes of real and imaginary parts also (Table I) of the bispectrum of case II. The quantitative significance of changes in sign and magnitude cannot be understood now as knowledge on real and imaginary parts is very meagre.

Acknowledgement

The author thanks Dr J.S. Sastry for encouragement.

References

- 1 Lake B M & Yuen H C, *J Fluid Mech*, 88 (1978) 33.
- 2 Varkey M J, *Indian J Mar Sci*, 17 (1988) 181.
- 3 Kim Y C & Powers E J, *IEEE Transactions on Plasma Sci*, PS-7 (1979) 120.
- 4 Varkey M J, An interpretation of nonlinearity in wind generated ocean surface waves (Communicated to *Indian J Mar Sci*).